

IMPROVED PERFORMANCE OF FILAMENT-WOUND COMPOSITE DRIVE SHAFTS WITH NEXT GENERATION INORGANIC NANOPARTICLE-FILLED EPOXY RESINS

Ambuj Sharma, James Nelson, Wendy Thompson, Douglas Goetz, Jesse Mack, Brett Beiermann,
Amit Patel, Jay Lomeda, Paul Sedgwick
3M Advanced Composites, Aerospace and Commercial Transportation Division
3M Center, St. Paul, MN 55144

Travis Gorsuch, Dave Knauff, Scott Neubauer
QA1 Advanced Materials Division
Lakeville, MN 55044

ABSTRACT

Previous work explored the impact of high matrix modulus on the design and performance of filament wound drive shafts [1-3]. In that research high modulus was accomplished by incorporating high loadings of surface-functionalized nanoscale silica particles into a low-viscosity epoxy winding formulation. Increased lamina transverse and shear stiffness were shown by calculation and experiment to translate into increased shaft longitudinal and hoop stiffness for a fixed winding pattern and fiber content. The resulting increase in shaft torsional strength governed by torsional buckling was demonstrated. Design equations were exercised to demonstrate the impact on optimization of composite shaft design.

In the present study next generation inorganic nanoparticle-filled epoxy matrix resin is shown to improve the strength of filament-wound composite drive shafts. High loadings of surface-functionalized nanoscale calcite particles are employed. First, neat resin properties for this technology are reported in order to demonstrate the range and balance of properties that are achievable. Important composite matrix resin mechanical properties including modulus and fracture toughness showed significant, generally monotonic improvement with increasing nanoparticle concentration. Desirable changes in coefficient of thermal expansion, cure exotherm, and hardness were also measured. Then the effect of increased matrix stiffness on shaft strength is demonstrated using sub-scale (ca. 25 mm diameter) $[\pm 40]_{2S}$ shafts as well as full-scale (ca. 74 mm diameter) shafts with a $[\pm 30/\pm 30/\pm 10/\pm 10/\pm 75]$ winding pattern. These data confirm that the new material technology can significantly improve the performance of composite structures where transverse and shear stiffness are important.

1. INTRODUCTION

1.1 Background

The translation of desirable fiber properties into composite material properties is dictated by the matrix and the fiber/matrix interface. The role of the matrix in the performance of fiber-reinforced polymer matrix composites is both enabling and limiting. Load transfer into the high modulus, high strength fibers, achieving low density for high specific strength and modulus, processing into net shape parts, and desirable anisotropy of composite lamina allowing unique design possibilities

all depend on the matrix. However, polymer matrix materials also limit the stiffness and strength in “off-axis” directions of laminae, control impact resistance, influence residual stresses through cure shrinkage and coefficient of thermal expansion mismatches with the fibers, and determine the temperature and moisture limits for composite use.

Epoxy resins are widely used as matrix resins because of their balance of thermomechanical properties and processing characteristics. A range of chemistries and commercial toughness modifiers makes this a very tailorable class of thermosetting polymer. However, the stiffness of epoxy matrix materials without inorganic particle modification is typically below 4 GPa. Introduction of rubbery second phase particles to increase fracture resistance reduces the matrix stiffness from the unmodified value. However, incorporation of a high volume fraction of inorganic particles can increase matrix modulus beyond the range achievable with any unoriented polymer. The use of surface-functionalized, low aspect ratio particles allows high loading while maintaining low viscosities needed for composite processing while increasing fracture resistance [4]. Nanoscale particles are needed to avoid particle filtration during fiber impregnation and to present a homogeneous mechanical environment for the reinforcing fibers [5, 6]. For such matrix modifications, the surface-modified nanoparticle must impart increased fracture toughness in order to avoid decreasing the fracture energy of the system. Notably, this has been observed with nanosilica-enhanced matrix resins where the fracture mechanisms appear to be similar to second-phase rubber particle toughening rather than the characteristic crack pinning mechanism usually associated with hard particle toughening⁷.

Inorganic nanoparticle enhancement of matrix resins has been demonstrated to improve matrix resin properties that translate into improvements in fiber-reinforced composite processing and properties. The incorporation of spherical nanoscale amorphous silica has been studied extensively. The present investigators have demonstrated the benefits of incorporating a high loading (up to 45 wt%) of nanoscale silica into epoxy matrix materials for unidirectional carbon fiber prepregs for both 121 °C (250 °F) and 177 °C (350 °F) curing [5, 6]. Additionally, neat resin and carbon-fiber composite properties of nanosilica-modified epoxy and bismaleimide resins designed for composite tooling applications were studied [8]. Nanosilica-containing, low viscosity resins, suitable for filament winding processes, have been studied for use in composite overwrapped pressure vessels [4]. In these studies composite matrix resin mechanical properties including modulus and fracture toughness showed significant, monotonically increasing improvement with increasing nanosilica concentration. Desirable changes in coefficient of thermal expansion, cure exotherm, and hardness were also measured. Silica concentration levels did not adversely affect the cured glass transition temperature or composite processing. Properties of carbon fiber laminates made with unidirectional prepregs or with fabrics of varying silica loading levels revealed significant improvements in compression strength, in-plane shear modulus, and 0° flexural strength. In general, the benefit of matrix modification with nanosilica is increased with increased loading levels.

1.2 The Effect of Inorganic Nanoparticle-Modified Epoxies on Drive Shaft Performance

1.2.1 Previous Work: Nanosilica

Previous work explored the impact of high matrix modulus on the design and performance of filament wound drive shafts [1-3]. In that research high modulus was accomplished by incorporating high loadings of surface-functionalized nanosilica into a low-viscosity epoxy

winding formulation. Increased lamina transverse and shear stiffnesses were shown by calculation and experiment to translate into increased shaft longitudinal and hoop stiffnesses for a fixed winding pattern and fiber content. The resulting increase in shaft torsional strength governed by torsional buckling was demonstrated. Design equations were exercised to demonstrate the impact on optimization of composite shaft design.

1.2.2 Current Study Objectives

In the present study the effect of next generation inorganic nanoparticle-filled epoxy matrix resin on the strength of filament-wound composite drive shafts is investigated. High loadings of surface-functionalized nanoscale calcite particles are employed to significantly alter the matrix properties, especially modulus. First, neat resin properties for a range of particle content are reported in order to demonstrate the range and balance of properties that are achievable. Three cure chemistries are used in these concentration studies. Important composite matrix resin properties are reported including modulus, fracture toughness, coefficient of thermal expansion, cure exotherm, cure shrinkage, and hardness. Second, the translation of increased matrix stiffness on shaft strength is investigated using sub-scale (ca. 25 mm diameter) $[\pm 40]_{2S}$ shafts as well as full-scale (ca. 74 mm diameter) shafts with a $[\pm 30/\pm 30/\pm 10/\pm 10/\pm 75]$ winding pattern.

1.2.3 Next Generation Inorganic Particle Technology

The material technology used for the present study is based on surface-functionalized nanoscale calcite. Various forms of calcium carbonate are commonly used as fillers for polymers and low-cost fiber composites such as sheet molding compounds (SMC). The features that distinguish the particles used in this study are 1) surface functionalization that enables low viscosity needed for composite processing and polymer/particle interactions needed for superior mechanical properties, and 2) particle size distribution enabling impregnation of the continuous fiber without filtration. To illustrate the latter capability, a pressure filtration experiment was conducted. Four layers of dry unidirectional carbon fiber fabric (Saertex fabric style S80CU990-00151, Toray T700 carbon fibers) were stacked in a $[0/90/-45/+45]$ degree sequence. Epoxy resin (Epon 826, Hexion) with amine curative (Ethacure 100, Albemarle) that was modified with 35 wt% nanocalcite was infused at room temperature through the thickness of the fabric stack. The resulting impregnated material was thermally cured. Figure 1 shows a cross-section of the cured laminate. The concentration is uniform from the top of the laminate to the bottom, confirming that the nanoscale particles were not filtered out during infusion.

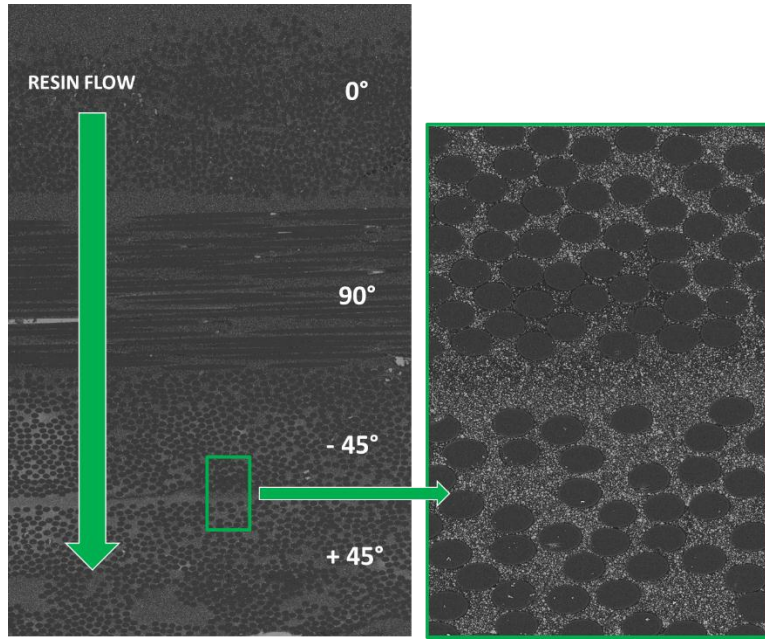


Figure 1. Cross-section of vertically infused transfer molded laminate demonstrating uniform distribution of nanocalcite after infusion processing.

2. THEORY OF DRIVE SHAFT DESIGN

The engineering constants of a thin-walled hollow tube often considered in design of a drive shaft are its axial, hoop, and shear moduli. Of the three moduli, the axial and hoop relate to stability against torsion buckling and lateral vibrations and the shear modulus is important for torsional vibrations. There are various mathematical treatments available in the literature for determining the buckling torque and flexural and torsional vibration characteristics of thin-walled hollow tubes [9-14]. In the present paper only the strength of filament wound tubes is considered. Several treatments of shaft torsional buckling are available that account for various situations, such as shaft slenderness. Equation 1 is an example expression for critical buckling torque given here to illustrate the dependence of the buckling torque on the axial and hoop moduli as well as the geometric characteristics of the shaft. It is empirically-derived, but has also been examined using the finite element method [11].

$$T_{buckling} = \frac{1.854}{\sqrt{L}} \times E_x^{0.375} \times E_\theta^{0.625} \times t^{2.25} \times D^{1.25} \quad (1)$$

where E_x and E_θ are the elastic modulus in the axial and hoop direction of the composite tube respectively, t is wall thickness of the tube, D is the diameter of the mid-plane of the tube wall, and L is the length of the tube.

A key concept for present study is that the axial and hoop moduli are dependent not only on the winding pattern, but also on the matrix modulus that strongly affects lamina transverse and shear stiffnesses. As previously noted, the modulus values of various conventional matrix resins are similar, but high loading of stiff inorganic nanoscale particles can be used to greatly increase the

effective matrix modulus, which in turn significantly increases ply transverse and shear stiffnesses, the laminate stiffnesses, and the engineering moduli of the shaft for a given winding pattern [1-3].

3. EXPERIMENTATION

3.1 Materials and Resin Sample Preparation and Testing

Resin samples were generated by dilution of an epoxy blend having 60 wt% nanocalcite of nominal particle size 400 nm in Epon 826 (Hexion). The initial calcite contents of this series of uncured resins were 60, 48, 32, and 16 wt%. A control sample containing no nanocalcite was also made. The pre-warmed (49 °C), nanocalcite-filled epoxies were blended with 3 wt% (relative to the epoxy component) of Dicyanex 1400B (Air Products) and 3 wt% Omniscure-U24 (Emerald Performance Products) using a DAC 600 SpeedMixer (Flacktek) at 2350 rpm for 45 seconds to produce well-dispersed blends. These blends were degassed under vacuum for 3-5 minutes prior to being poured into appropriate molds for neat resin tensile testing, dynamic mechanical analysis (DMA), and determination of hardness, coefficient of thermal expansion (CTE), density, and fracture toughness. The samples were cured in a forced air oven for 1 hour at 90 °C and then for an additional 2 hours at 150 °C. Neat resin castings were also cured using Lindride 36V (Lindau Chemical) at a 0.95 charge of anhydride to epoxide functionality with the same cure schedule as used for the dicy cure. Additional samples were cured with Ethacure 100 amine (Albemarle) at a 1.1 overcharge of amine to epoxide functionality. These samples were cured in a forced air oven using a sequence of 1 hour at 75 °C, 2 hours at 125 °C, 2 hours at 150 °C, and 1 hour at 165 °C. The cured resin specimen preparation and testing methods used to obtain neat resin properties have been described previously [1-3]. All testing was conducted under ambient laboratory conditions.

3.2 Filament Wound Carbon Fiber Tube Production and Specimen Preparation

Laboratory scale shafts were wound by 3M using T700SC-24K-50C Torayca® carbon fiber (Toray) and both 48 wt% calcite resin and the corresponding unfilled control resin, which was Epon 826 bisphenol-A epoxy (Hexion) cured with 3 wt% (relative to the epoxy component) of Dicyanex 1400B (Air Products) and Omniscure-U24 (Emerald Performance Products) as described above. The tubes (nominal dimensions of 25.4 mm inner diameter, 0.9 mm thickness) were wound on an aluminum mandrel. A $[\pm 40]_{2S}$ winding pattern was used. This simple pattern was chosen in order to illustrate the role of matrix modulus on tube strength. After winding, the tubes were wrapped with shrink tape. The tubes were cured at 90 °C for 1 hour and 150 °C for 2 hours. The cured tubes were trimmed to approximately 500 mm length and steel inserts with lugs for torsion loading were bonded to both ends for load introduction during a quasi-static torsional test. The bonding length of each insert was ca. 25 mm. In order to control the bondline thickness, a small amount of 125 micron diameter glass beads was added to the epoxy adhesive that was used for the bonding.

Winding of full scale drive shafts was conducted by QA1 using T700SC-12K Torayca® fiber and both 48 wt% calcite and the corresponding unfilled control resin. The control resin was Epon 826 bisphenol-A epoxy (Hexion). The Dicyanex 1400B (Air Products) and Omniscure-U24 (Emerald Performance Products) were blended at 3 wt% (relative to the epoxy component). Winding was done on an aluminum mandrel with a $[\pm 30/\pm 30/\pm 10/\pm 10/\pm 75]$ winding pattern. The tubes had nominal dimensions of 7.37 cm inner diameter and 1.75 mm wall thickness. This geometry and winding pattern were chosen to represent the diameter and winding angles typical in vehicle drive

shafts while considering practical testing constraints. After winding, the tubes were covered in shrink tape with suitable tension. The tube was cured using a multistep cure of 90 °C for 1 hour and 150 °C for 2 hours. A section ca. 0.53 m long was cut from each tube, then a proprietary bonding procedure developed by QA1 was used for bonding aluminum inserts to both ends for load introduction during a quasi-static torsional test.

3.3 Test Procedure for Laboratory Scale Carbon Fiber Tubes

Torsional strengths of the laboratory scale (2.54 cm inner diameter) tubes were determined using the test setup shown in Figure 2. Lugs on the bonded inserts engaged a fixed grip on one end and a movable grip supported by ball bearings on the other end. The movable grip was attached to a digital torque wrench with peak torque capture capability. Monotonically increasing torsional loading was performed manually until tube failure.

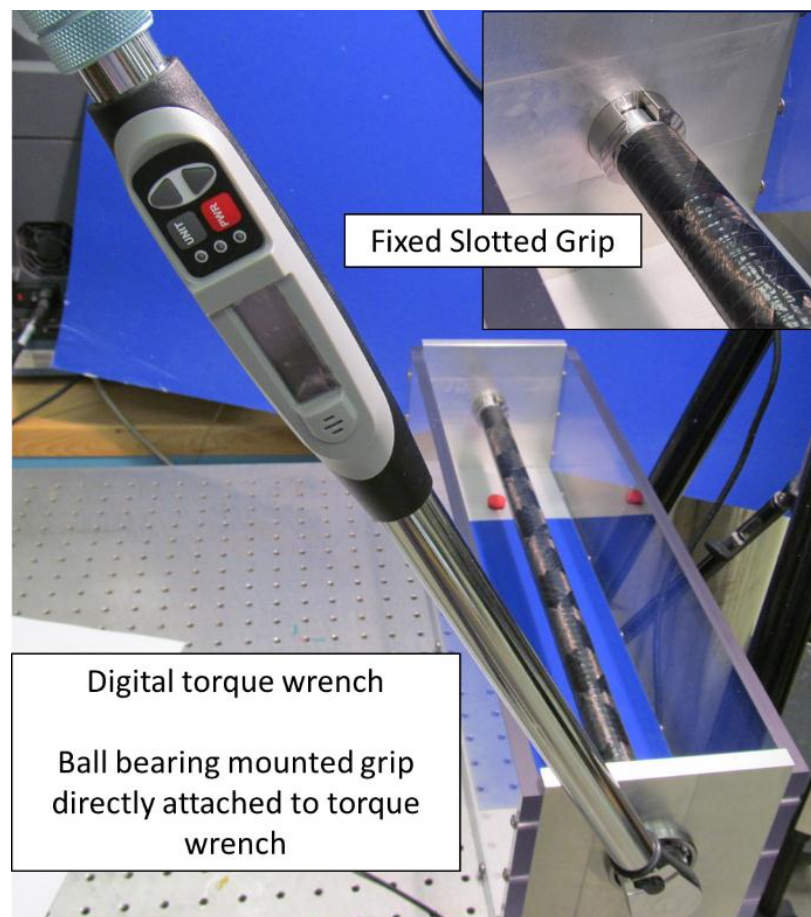


Figure 2. Test setup for torsional strength testing of laboratory scale tubes

Digital Image Correlation (DIC) was used for representative tubes to image deformations during loading. The intent was to verify torsional buckling as the primary failure mechanism. It is known that for thin walled structures, global buckling, local buckling, and material failure are all possible failure modes [9-14]. The concern of the designer is to have confidence which mechanism governs failure—that is, which occurs at the lowest load, and to ensure that the other possible failure mechanisms are not expected to occur at loads near that predicted failure load, even in

consideration of variations in material strength or part manufacturing. Here, direct observation of torsional buckling deformations just before part failure is used to verify that the primary failure mechanism is torsional buckling, which is expected to be dependent indirectly on matrix modulus. At buckling, the peak load is reached and large subsequent deformations lead to actual material failure. A speckle pattern for DIC was applied to the mid-section of the tubes ca. 140 mm long by first applying a thin coat of flat white paint uniformly to the area and then applying a random speckle pattern using black paint. Image pairs were captured throughout the tube loading using two CCD cameras. A DIC system and software by Correlated Solutions, Inc. was used.

3.4 Test Procedure for Full Scale Carbon Fiber Tubes

The testing of full scale shafts was conducted by QA1 in Lakeville, Minnesota using a custom-designed hydraulic torsional machine. The applied torque and resulting twist angle were recorded as the torque was increased monotonically to shaft failure. For this test, the ultimate torque is defined as the maximum load sustained by the specimen before complete failure.

4. RESULTS

4.1 Neat Resin Properties

Tables 1-4 summarize neat resin data for this concentration study.

Table 1. Resin Processing Data for Dicy/Urea-cured Nanocalcite Epoxy Matrix Resin.

Calcite (wt%)	Complex Viscosity @ 25°C (Pa-s)	Minimum Complex Viscosity @ 130°C (Pa-s)	Cure Exotherm (J/g)	Cure Exotherm Reduction (%)	Cure Shrinkage (%)
0	2.0	2.0×10^{-2}	557	0	0.54
16	5.0	2.0×10^{-2}	480	14	0.45
32	10.1	3.0×10^{-2}	391	30	0.38
48	25.2	8.0×10^{-2}	300	46	0.28
60	40.0	1.4×10^{-1}	209	62	0.18

Table 2. General Cured Resin Data: Dicy/Urea-cured Nanocalcite Epoxy Matrix Resin.

Calcite (wt%)	Barcol Hardness (H _B)	CTE (μm/m/°C)		Density (g/cc)	Calcite Volume Fraction (%)
		-25-25°C	25-75°C		
0	30	58.0	69.7	1.192	0
16	36	49.4	57.4	1.302	7.9
32	45	45.7	52.4	1.430	17.0
48	53	36.9	42.0	1.602	29.3
60	64	33.1	36.0	1.758	40.4

Table 3. Resin Mechanical Property Data: Dicy/Urea-cured Nanocalcite Epoxy Matrix Resin.

Calcite (wt%)	T _g (°C)	Tensile Properties			Fracture Toughness (MPa-m ^{1/2})	Critical Energy Release Rate (J/m ²)
		Modulus (GPa)	Strength (MPa)	Strain (%)		
0	140	2.8	80.0	5.1	0.53	86
16	138	3.6	71.7	3.0	0.71	120
32	140	4.6	60.0	1.9	0.78	113
48	142	6.6	57.2	1.1	0.88	100
60	140	8.2	55.8	0.8	0.82	70

Table 4. Additional Resin Mechanical Property Data: Anhydride-cured (36V) and Amine-cured (E100) Nanocalcite Epoxy Matrix Resin.

Calcite (wt%)	Curative (charge)	T _g (°C)	Tensile Properties			Fracture Toughness (MPa-m ^{1/2})	Critical Energy Release Rate (J/m ²)
			Modulus (GPa)	Strength (MPa)	Strain (%)		
0	36V (0.95)	124	3.1	85.2	5.5	0.58	93
35	36V (0.95)	124	4.5	66.9	2.0	0.76	110
45	36V (0.95)	124	5.9	59.9	2.0	0.84	102
0	E100 (1.1)	165	3.0	47.2	2.6	0.69	136
45	E100 (1.1)	168	4.5	50.6	2.3	1.68	537
53	E100 (1.1)	168	5.4	50.4	1.8	1.82	525

4.2 Effect of Calcite Concentration on Processability and Part Fabrication

Resin viscosity during curing is an important criterion for resin systems. Rheometric analysis using viscosity vs. temperature profiles was used to quantify viscosity as it depends on calcite content. In Table 1 is shown the viscosity of each of the resins at room temperature and 130°C, corresponding to winding and an arbitrary higher temperature representative of the cure. Viscosity increases with increasing particle content, but remains in a processible range. In subsequent sections of this paper, a 48 wt% sample was utilized in a filament winding process to make low-void laminates from the filled formulation.

The cure exotherm as a function of calcite content is shown in Table 1. There is a reduction of cure exotherm with increasing calcite content. In a previous study of nanosilica-modified dicy-cured resins, the cure exotherm was found to be reduced proportionally to the organic weight fraction [5]; the inorganic nanoparticle acts as an inert filler. The same effect is seen here. For example, the reduction of cure exotherm is reduced by about 62% by the addition of 60 wt% nanocalcite. Nanocalcite lowers the extent of exotherm during cure by simply reducing the amount of curable resin present. This may be very important for the fabrication of thick parts where heat

management during cure is crucial. Also shown in Table 1 are the cure shrinkage values which show the trend of reduced cure shrinkage with increased calcite content. Both of these features are desirable for composite fabrication.

4.3 Effect of Calcite Concentration on Cured Resin Properties.

Reduced coefficient of thermal expansion (CTE) is desirable for composite matrix materials in order to reduce thermal stresses and part distortion. The reduction of CTE with increasing calcite concentration is shown in Table 2. For example, incorporation of 48 wt% nanocalcite lowered the CTE by 36 to 40% over the temperature ranges examined. Additionally, increasing calcite incorporation leads to an increase in surface Barcol hardness (Table 2). The high hardness enhances durability and part surface quality.

Density measurements were conducted on cured resin samples ranging from 0-60 wt% nanocalcite and results are displayed in Table 2. The inclusion of nanocalcite in resins increases the density of the resultant system because the density of calcite is higher than that of the base resin. The measured densities and weight fractions of calcite can be used to verify the nominal effective density of these surface-functionalized particles is ca. 2.7 g/cc. Typical carbon fiber parts have fiber volume fractions of about 60%, so the increase in density of composites with nanocalcite modification is about 7% at 35 wt% loading. As has been demonstrated, even with increased density the gain in composite properties due to nanoparticle matrix modification offer composite designers latitude in eliminating carbon fiber and other weight- and cost-saving strategies [3]. These can result in an overall reduction in part weight for equal strength or stiffness. Also listed in Table 2 are the corresponding volume % of calcite calculated using the measured densities.

Cured resin tensile tests were performed to directly measure the resin tensile modulus. Table 3 lists the tensile modulus as well as the average stress and strain at failure. At the 48 and 60 wt% levels of nanocalcite, the tensile modulus was 236 % and 293 % of the control resin modulus. The failure stress and strain were reduced with increasing calcite content. The flaw-sensitive nature of tensile testing suggests that the reduction seen in tensile testing is greater than the in-situ reduction in composites application. For higher loadings, increased calcite content appeared to produce similar strength levels with reduced failure strains for this resin system.

Results of resin fracture testing are given in Table 3. The critical plane-strain stress intensity factor, K_{IC} , increased with increasing nanocalcite content until the content exceeded 48 wt%. The incorporation of 48 wt% calcite increased K_{IC} by about 66%. Critical energy release rate is also reported in Table 3. Values were calculated from K_{IC} and tensile modulus assuming a Poisson's ratio of 0.38. Both fracture toughness and fracture energy were higher than the unfilled control at all calcite levels except 60 wt%. This confirms that the increase in fracture resistance due to the incorporation of surface-functionalized calcite is sufficient to prevent embrittlement of the resin even as the modulus is dramatically increased.

Additionally, calcite modified epoxy formulations were evaluated with aromatic amine and anhydride curatives according to the ratios and calcite loadings levels reported in Table 4 in order to display the utility of this nanoparticle approach for other curative systems. Anhydride-cured nanocalcite epoxy at 45 wt% calcite displayed a 44% increase in fracture toughness, while simultaneously increasing tensile modulus by 90% over the anhydride-cured control resin. The corresponding aromatic amine-cured nanocalcite epoxy at 53 wt% calcite displayed an 80%

increase in tensile modulus while simultaneously increasing fracture toughness by 164 % over the aromatic amine-cured control resin. Critical energy release rate reported in Table 4 were calculated from K_{IC} and tensile modulus assuming a Poisson's ratio of 0.38. Both fracture toughness and fracture energy were higher than the unfilled control at all calcite levels tested. Note that the effect of nanocalcite modification on the amine system fracture resistance was much greater than for the dicy or anhydride-cured resins. Not only is the resistance maintained as modulus is increased, but it is greatly increased—e.g., giving about four times increase in the critical energy release rate for 45 wt% nanocalcite. The glass transition temperatures reported in Tables 3 and 4 show that the incorporation of nanocalcite did not affect the T_g for any of the three curatives used.

4.4 Laboratory Scale Tube Strength

Five tubes made using the unfilled control epoxy resin were tested to failure. The average torque for failure was 88.0 N-m with a standard deviation of 1.5 N-m. Five tubes made using 48 wt% nanocalcite-modified epoxy were tested to failure. The average torque for failure was 115.5 N-m with a standard deviation of 5.4 N-m. The increase in the average failure torque was 31.4%.

For all tubes, local ovalization of the cross-section due to torsional buckling could be observed just before peak load. This behavior is clearly seen in the DIC measurements of displacements and shape. In Figure 3 representative results are shown. The images show color contour plots of vertical displacements superimposed on the shape of the portion of the tube that was decorated with a speckle pattern. Images (a), (b), and (c) are successive data captured just before peak load for one of the calcite epoxy tubes. In image (a) the shape is cylindrical (the plot's vertical scale factor gives the impression of a parabolic shape for the half-cylinder). The contour lines of displacement rise to the left because of the twisting of the tube. Image (b) corresponds to a slightly higher torque. Buckling has begun, and the shape is no longer cylindrical, but has become saddle-shaped. Displacements in the convex part of the saddle are negative. Image (c) is from just before failure, and the saddle has become deeper, reflecting continuing collapse.

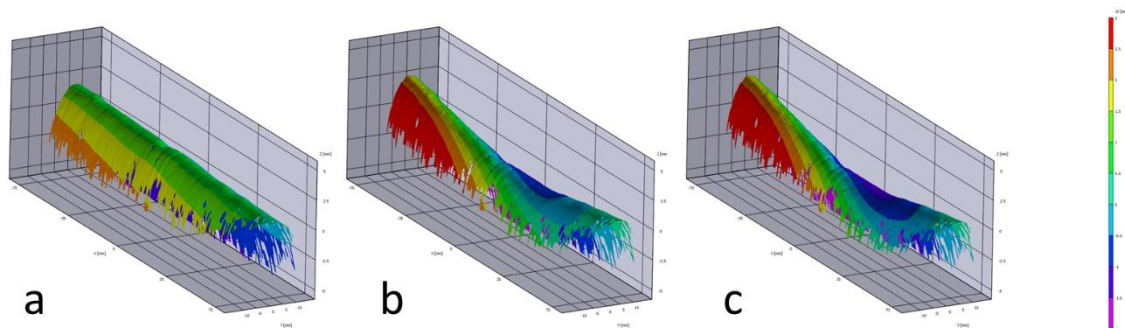


Figure 3. Vertical displacements in laboratory-scale tube confirming torsional buckling. Increasing torsional displacement (a) to (b) to (c). Displacement color contours range from greater than 2.5 mm (Red) upward to deflections downward greater than 1.5 mm (Purple).

Similar sequences of data were captured from all DIC performed, confirming failure by torsional buckling. For these tubes, the effect of matrix resin modification on torsional strength was due to the effect on hoop and longitudinal stiffness, which in turn affects buckling, as opposed to

increasing laminate compression strength, which is also known to result from nanoparticle modification of matrix resins [5,6,8,15].

4.5 Full Scale Tube Strength

Figure 4 shows the torque-angular displacement curves for the full-scale tubes. Note that for this winding pattern the torsional stiffness represented by the slope of the curves is the same for the control and calcite-modified epoxy tubes. Both curves rise to a maximum, then the torque drops to a lower level as the angular displacement increases before a sudden and final load drop at failure. This characteristic behavior is expected for buckling. The peak torque for the control was 2363 N-m and for the nanocalcite modified shaft 2862 N-m. The increase in peak torque for the shaft made with nanocalcite modified epoxy is 21%.

The locus of failure for each of the two shafts is shown in Figure 5. Both failed away from the ends with lines of material separation at roughly 30° terminated by segments at roughly 75°, following two of the directions of the fiber layup. The direction of the applied torque is such that the material along the dashed line in Figure 5 experienced shear and compression. It should be noted that peak shaft torque was reached before these failures developed. Shaft failure was by torsional buckling; the material failure pictured occurred after buckling and included not only the nominal shear and compression loads, but through-thickness bending stresses generated by the radial displacements of the collapsing cross-section. Similar to the laboratory-scale tubes, ovalization of the cross-sections each of the shafts could be seen just before failure.

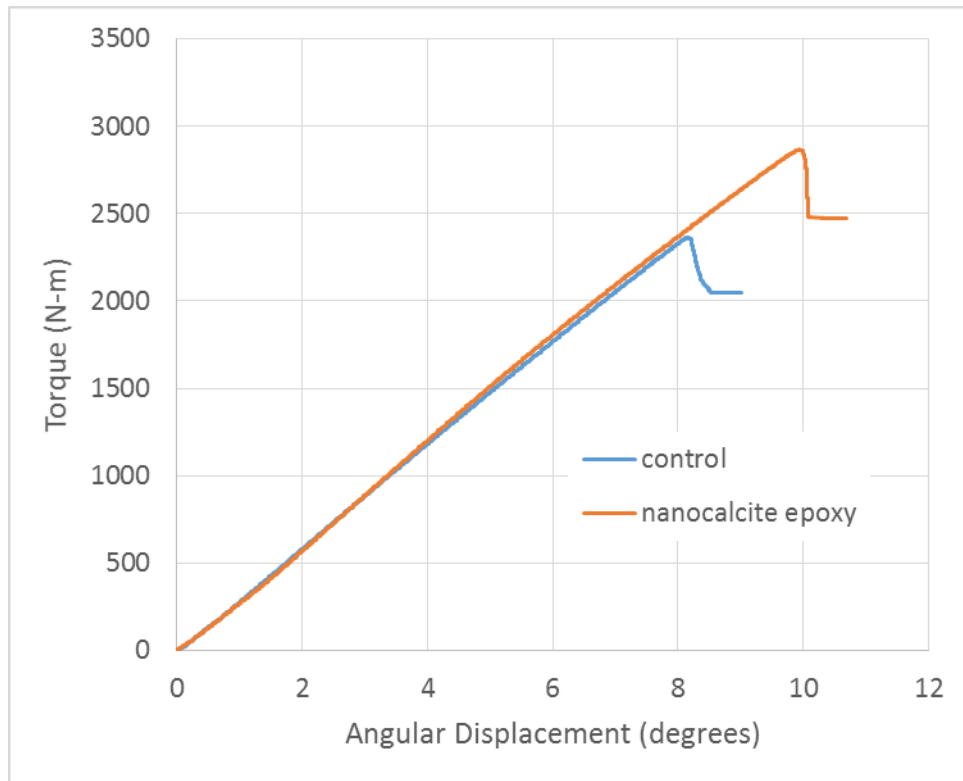


Figure 4. Torque vs. angular displacement for full scale shafts



Figure 5. Failed full scale shafts a) unmodified control b) 48 wt% calcite-modified epoxy

In order to verify that the control shaft was a good comparison for the calcite-modified shaft, cross-sectioning and micrographic analysis were performed on both shafts. Sections were cut in locations away from the damaged material. These were mounted in epoxy and polished. Fiber volume fractions, wall thickness, and fiber directions were determined by image analysis using techniques previously described [1]. Fiber volume fraction was estimated to be 61.5 vol% for the control shaft and 58.2 vol% for the calcite-modified shaft. Fiber angle analysis showed winding angles of $\pm 41^\circ/\pm 13^\circ/\pm 69^\circ$ for the control shaft and $\pm 32^\circ/\pm 11^\circ/\pm 77^\circ$ for the calcite-modified shaft. The average thickness was measured to be 1.685 mm for the control shaft and 1.836 mm for the calcite-modified shaft. From modeling of buckling torque the differences in fiber volume fraction and angles are not expected to make a significant difference in failure torque (<1% difference), confirming the validity of the comparison to the control shaft.

It is important to note that matrix modulus is one of several important material and design variables contributing to torsional strength. The interactions of these variables have been explored previously [3]. The present experimental comparison illustrates how for a given design, increasing the modulus of the matrix resin can cause a significant increase in performance. Previous work has illustrated strategies for using this increased performance in the shaft design process [1-3].

5. SUMMARY AND CONCLUSIONS

In the present study next generation inorganic nanoparticle-filled epoxy matrix resin is shown to improve the strength of filament-wound composite drive shafts. In the first part, neat resin properties for this technology are reported to demonstrate the range and balance of properties that are achievable

5.1 Matrix Resin Properties

The modification of epoxy matrix resins with surface-functionalized nanoscale calcite particles was shown to produce significant, monotonic improvement in matrix modulus, a key matrix property affecting the torsional buckling strength of filament-wound shafts. Along with the increase in modulus, the fracture resistance of the resin was increased above that of the base resin. Desirable changes in cure exotherm, coefficient of thermal expansion, cure shrinkage, and hardness were also measured. These additional property improvements were generally increased with increasing particle content up to high loadings. Modest increases in room temperature viscosity were measured, but viscosity was suitable for filament winding even for high particle fractions. As expected, density increased with increasing inorganic particle content. Desirable resin modifications were seen for dicy/urea, anhydride, and amine cures. Glass transition temperatures for the filled resins were unchanged from those of the base resins. Fracture resistance for the amine-cured resin tested was improved more than for the others.

5.2 Effect of Matrix Resin Properties on Torsional Strength of Filament-Wound Shafts

The effect of increased matrix stiffness on shaft strength was demonstrated using sub-scale (ca. 25 mm diameter) $[\pm 40]_{2S}$ shafts as well as full-scale (ca. 74 mm diameter) shafts with a winding sequence of $[\pm 30/\pm 30/\pm 10/\pm 10/\pm 75]$ by direct comparison of the strength of shafts made with an unfilled control and made with the same resin modified with 48 wt% nanocalcite. The sub-scale shafts showed an average increase in failure torque of 31%. The failure mode was confirmed to be torsional buckling by DIC measurements. The increase in peak torque for the 74 mm diameter shaft made with nanocalcite modified epoxy over the strength of the control was 21%.

The next generation nanocalcite technology has been shown to cause a significant increase in shaft torsional strength for a given winding pattern and geometry. It therefore presents designers with the means of optimizing shaft strength and enables design optimization for cost and other shaft performance characteristics.

6. ACKNOWLEDGEMENTS

The authors would like to thank Lindy Bowen and James Thorson of 3M's Corporate Research Process Laboratory for resin processing assistance and Melissa Scoles at QA1.

7. REFERENCES

1. Nelson, J.M., et al. "Nanosilica-Modified Epoxy Resins for Use in Filament-Wound Drive Shaft Applications." *CAMX Conference Proceedings*. Orlando, FL, Oct 13-16, 2014. *CAMX – The Composites and Advanced Materials Expo*. CD-ROM.
2. Nelson, J.M., et al. "Nanosilica-Modified Epoxy Resins for Use in Filament-Wound Drive Shaft Applications." *Plastics in Motion 2015*, Dearborn, MI June 1-4, 2015.
3. Sharma, A., et al. "The Impact of Nanosilica-Modified Epoxy Resins on the Design and Performance of Filament-Wound Drive Shafts." *CAMX Conference Proceedings*. Dallas, TX, Oct 26-29, 2015. *CAMX – The Composites and Advanced Materials Expo*. CD-ROM.

4. Thunhorst, K., et al. "Nanosilica Concentration Effect on Epoxy Resins and Filament-Wound Composite Overwrapped Pressure Vessels." *Proceedings of the International SAMPE Tech. Conf.* Long Beach, CA, May 23-26, 2011. Society for the Advancement of Materials and Process Engineering.
5. Hackett, S.C., et al. "The Effect of Nanosilica Concentration on the Enhancement of Epoxy Matrix Resins for Prepreg Composites." *Proceedings of the International SAMPE Tech. Conf.* Salt Lake City, UT, Oct. 11-14, 2010. Proc. Society for the Advancement of Materials and Process Engineering.
6. Nelson, J.M., et al. "Development of Nanosilica-Epoxy Matrix Resins for High Temperature Prepreg Composites." *Proceedings of the International SAMPE Tech. Conf.* Long Beach, CA, May 23-26, 2011. Society for the Advancement of Materials and Process Engineering.
7. Liang, Y.L. and Pearson, R.A. "Toughening Mechanisms in Epoxy-Silica Nanocomposites (ESNs)." *Polymer* 50 (2009): 4895-4905.
8. Nelson, J.M., et al. "The Development of Nanosilica-Modified Tooling Prepregs: A Progress Review and New Advances." *CAMX Conference Proceedings*. Orlando, FL, Oct 13-16, 2014. *CAMX – The Composites and Advanced Materials Expo*. CD-ROM.
9. Bert, C.W., and Kim, C-D. "Analysis of Buckling of Hollow Laminated Composite Drive Shafts." *Composites Science and Technology* 53 (1995): 343-351.
10. Bauchau, O.A., Krafchack, T.M., and Hayes, J.F. "Torsional Buckling Analysis and Damage Tolerance of Graphite/Epoxy Shafts." *Journal of Composite Materials* 22 (1988): 258-270.
11. Shokrieh, M.M., Hasani, A., and Lessard, L.B. "Shear Buckling of a Composite Drive Shaft Under Torsion." *Composite Structures* 64 (2004): 63-69.
12. Lim, J.W., and Darlow, M.S. "Optimal Sizing of Composite Power Transmission Shafting." *Journal of the American Helicopter Society* 31-1 (1986): 75-83.
13. Weaver, P.M. "Design of Laminated Composite Cylindrical Shells under Axial Compression." *Composites: Part B* 31 (2000): 669-679.
14. Weaver, P.M., Driesen, J.R., and Roberts, P. "Anisotropic Effects in the Compression Buckling of Laminated Composite Cylindrical Shells." *Composites Science and Technology* 62 (2002): 91-105.
15. Uddin, M.F., Sun, C.T. "Strength of Unidirectional Glass/Epoxy Composite with Silica Nanoparticle-Enhanced Matrix." *Composites Science and Technology* 68 (2008): 1637-1643.